Available online at www.sciencedirect.com

ScienceDirect

journal homepage: www.elsevier.com/locate/he

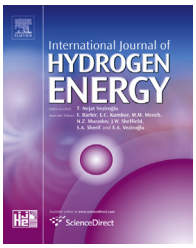

Energy and provision management study: A research activity on fuel cell design and breadboarding for lunar surface applications supported by European Space Agency

Orazio Barbera [a,*], *Filippo Mailland* [b], *Scott Hovland* [c], *Giosuè Giacoppo* [a]

[a] *CNR – ITAE, Consiglio Nazionale delle Ricerche, Istituto di Tecnologie Avanzate per l'Energia "Nicola Giordano", Italy*

[b] *CGS S.p.A. – Compagnia Generale per lo Spazio, Italy*

[c] *European Space Agency – ESTEC, The Netherlands*

ARTICLE INFO

Article history:
Received 11 March 2014
Received in revised form
30 June 2014
Accepted 3 July 2014
Available online 26 July 2014

Keywords:
Polymer electrolyte fuel cells
Pure reactants
Stack design
RFC
Space applications

ABSTRACT

This paper addresses the findings of the European Space Agency (ESA) study (Energy and Provision Management Study), performed by an Italian consortium, aimed at designing and breadboarding of an Energy Provision and Management system (EPM), based on Polymer Electrolyte Fuel Cell (PEFC) technology. The EPM has been developed for supporting space exploration applications, specifically for lunar surface missions. The fuel cell technology has been selected through a trade-off activity, and the power requirements of a Lunar Base (LB) power plant and a Pressurized Lunar Rover (PLR) have been identified. A synergetic design of EPM has been proposed for both the LB and the PLR. Finally three technological demonstrators have been designed, manufactured and tested: i) a 1 kW PEFC stack, ii) a stand-alone power system based on the developed stack, iii) a regenerative power system based on the stand-alone stack connected with a commercial electrolyser. The tests carried out on breadboards, have demonstrated the ability of fuel cell power systems to meet the requirements of future space missions.

Introduction

The provision and storage of energy is of vital importance for the success of both manned and robotic space exploration missions. A wide range of mission types (robotic, human, In Situ Resources Utilization (ISRU) etc.) with a variety of different environments exist; from interplanetary space, to the shadow of a lunar crater, to the attenuated and red-shifted lighting on the Martian surface. For this reason, different power requirements must be met, and consequently, different power systems have to be used: e.g. solar, nuclear, battery and fuel cell [1]. The major power system challenges in solar system missions are related to the location, solar irradiance, environment and radiation. These challenges can be met if the power systems have long life, high specific power and high

* *Corresponding author.*
E-mail address: orazio.barbera@itae.cnr.it (O. Barbera).
http://dx.doi.org/10.1016/j.ijhydene.2014.07.015

power capabilities, mass and volume efficiency, ability to operate in extreme environments, human rated safety and high reliability. The majority of space power generation systems use radioisotope and solar cells as power sources. Nuclear power systems use a radio isotope as heat source and a power converter to generate electric power from heat (Thermoelectric, Stiring, Thermo – photovoltaic) [2–4]. They are of key importance in dark and/or particularly cold environments, making them an enabling technology for many deep space and planetary missions [1]. Photovoltaic power systems are used on 99% of the space missions, especially in Earth and planetary orbital missions and in planetary surface missions. The capability of those systems ranges from 0.5 to 20 kW, the radioisotope power sources produce 4–5 W/kg with 6.5% of efficiency, the solar cells 30–60 W/kg and 9–26% of efficiency. Further development of these power sources is aiming to providing a significant increase in specific power: 500 W/kg in case of power solar arrays, 200 W/kg in case of nuclear systems. Moreover, operational capabilities, extreme temperature, high radiation and dusty environments tolerance, life, reliability and safety have to be enhanced. The described power generation systems are generally coupled with an energy storage system, that is used to provide primary electrical power to: launch vehicles, crew exploration vehicles, planetary probes, astronaut equipment, etc. Storage systems provide electrical energy during eclipse periods, satisfying peak power demands. The most important energy storage system technologies are primary batteries, rechargeable batteries and Polymer Electrolyte and Alkaline fuel cells, combined with an electrolyser (EZ) in a Regenerative Fuel Cell (RFC) energy storage system. At present, primary batteries are characterized by a specific energy of 100–250 Wh/kg and a mission life of 5–10 years. Rechargeable batteries are characterized by a specific energy of 8–100 Wh/kg, and life of 500–60000 cycles. Both of these technologies have limitation in operating temperature ranges and the radiation tolerance is not fully understood. Primary batteries generate a moderate specific energy, rechargeable batteries are heavy and bulky. For future planetary surface and orbital missions (i.e. Titan Saturn exploration mission, Mars exploration mission, Neptune orbiter, planned by 2018–2025), rechargeable batteries will have longer mission life (>15 years), higher specific energy (>150 Wh/kg), enhanced radiation tolerance and longer cycle life (>50000 cycles), primary batteries will have high specific energy (>600 Wh/kg) [2,3]. Considering the above discussed requirements, current power conversion and energy storage systems do not meet all future critical space mission needs. Because of the high energy density of Li-ion technology, which is expected to rise up to 160 Wh/kg, is attractive. However, even higher energy densities can be reached by fuel cells. Furthermore, the combination of hydrogen and oxygen is very promising to make an energy storage device with high energy density and to reuse the by-product water for the electrolysis reaction [5]. PEFC technology appears to be a promising technology for power generation in exploration missions, especially in situations involving the in-situ use of resources and large surface power plants, indeed, fuel cell systems have a potential for specific energy of >500 Wh/kg [6,1]. Also for space vehicle applications, PEFC technology offers major advantages over existing alkaline fuel cell technology. This includes enhanced safety, longer life, lower weight, improved reliability and maintainability, higher peak to-nominal power capability, compatibility with propulsion grade reactants, and the potential for significantly lower costs [7]. PEM – based RFCs have been proposed particularly in combination with solar arrays, due to their high energy density (400–600 Wh/kg). Primary Fuel cells (non-regenerative) are even more efficient than RFCs, providing energy density in the order of 600 Wh/kg to more than 1000 Wh/kg [1]. European space exploration takes place through the ESA [8], European industry and academia [9]. Among different space programs, the ESA's Aurora programme aimed at setting out a strategy for solar system exploration over the next 20 years. The programme and its principle were unanimously approved at the ESA council at Ministerial Level, held in Edinburgh (UK) in 2001. The final goal was to allow European astronauts to reach Mars by the end of the third decade of 21st century. Europe has visited the Red Planet and the Moon by Mars Express and Smart-1 robotic mission respectively. Similarly, ISS is giving Europe indispensable experience in human space flight for training humans to live in deep space for long periods of time. The technologies that are needed to explore the Red Planet with robots, and those necessary to sustain humans for years in hostile environments can be as diverse as: power and propulsion systems, life-support systems, long-term habitability module design, assembly in low earth orbit, rendezvous and docking in mars orbit, image recognition, automatic precision navigation, radiation protection, health monitoring, bio-protection. As part of Aurora programme, numerous studies have been carried out or are in progress: ISRU System and Technology Study, Energy Provision and Management Study, Superconductive Magnet for Radiation Shielding Study, Advanced Closed-Loop Systems (ACLS) for life support, MELiSSA (Micro-Ecological Life Support System Alternative), Black Water Treatment Breadboard and Exploration Robotics Requirements [10–13], to name a few. In this paper the activity of the EPM study is illustrated. On the basis of the discussed power requirements for future space exploration missions, a deep study and analysis on energy provision and management solutions has been performed, the activity focused on fuel cell technology.

In the next sections, the following item are described: a brief presentation of fuel cell, electrolysers and hydrogen storage technologies, the selection of the best technology for the EPM system via a trade – off analysis, the requirements and the sizing of energy provision and management systems for PLR and LB, the feasibility of the chosen technology by the designing, manufacturing and testing of three different demonstrators. The study has been performed under the ESA supervision, by an Italian consortium made up of CGS (Compagnia Generale per lo Spazio) and CNR – ITAE (National Research Council of Italy–Institute for Advanced Energy Technologies).

The fuel cell technology

Principles

Fuel cells (FCs) are electrochemical devices able to convert the chemical energy of a reaction directly into electrical energy. A

fuel cell recombines the reactants H_2 and O_2 and provides electrical power and water [14,15], the physical structure of a FC consists of an electrolyte layer in contact with two electrodes: a porous anode on one side and a porous cathode on the opposite side. Typically in a FC, hydrogen and oxygen are continuously supplied at the anode and cathode compartment respectively. At the two catalysed electrodes, fuel and oxidant, respectively gain and loss electrons, which are obliged to flow through an external circuit generating current, while charged particles moving from one electrode to another through the electrolyte. Table 1 provides a brief FC technology overview, where FC has been classified on the basis of the electrolyte type [16,17]:

The electrochemical process of any fuel cell can be ideally reversed, a given device optimized for operating in reverse mode is called an Electrolyser. Such a device uses electricity to split the water into two gases, H_2 and O_2. Three main technologies have been demonstrated to be operated in reverse mode, that can be distinguished according to the electrolyte they use: (i) alkaline electrolysers, with a liquid electrolyte; (ii) polymer electrolyte membrane (PEM) electrolysers, with an acidic solid ionomer electrolyte, (iii) high-temperature steam electrolysers, with a solid oxide electrolyte. The process is the same in all three technologies: water is fed to the electrochemical cell in which hydrogen evolves at the negative electrode (cathode) and oxygen at the positive electrode (anode) when a sufficiently high voltage is applied to the cell [18,19]. Fig. 1 sketches the operation of a PEM FC and an EZ:

Table 2 summarizes the described electrolyser technologies:

A regenerative fuel cell system uses EZ and FC to store and provide energy similarly to a rechargeable battery. The EZ provided with energy from an external source (solar arrays or wind turbines), can be used to store it as high pressure gases (hydrogen and oxygen) that can be reconverted into electricity by the fuel cell. The electrolyser and fuel cell functions can be integrated into a single stack (Unitized Regenerative Fuel Cell) or separated in two different devices (discrete, Regenerative Fuel Cell). Both configurations are illustrated in Fig. 2:

Unitized systems (URFC) are attractive in terms of reduced system mass and complexity due to the auxiliary sharing and the unified housing, otherwise, this implies some limitations in power production and reactants delivery. Moreover the bifunctional electrodes requires to be optimized for both oxygen reduction and water oxidation. Discrete systems, in order to store the gaseous fluids in reasonable volumes with minimal mass, operate the electrolyser portion of the system at significant pressures, for efficient high pressure electrolysis. And the fuel cell stack portion is operated at low pressure, for high efficiency power production. In an RFC system, the reactant storage aspects and in particular the hydrogen storage becomes very important. Hydrogen can be stored as (i) pressurized gas, (ii) cryogenic liquid, (iii) solid fuel as chemical or physical combination with materials, such as metal hydrides, complex hydrides and carbon materials. Basically, there are six possible methods to reversibly store hydrogen with a suitable gravimetric density [20,21] as Table 3 lists:

Selection of technologies for the EPM system

Trade-off analysis

Methodology overview

Presently, the technology development offers several types of fuel cells - based power systems, that could meet future requirements of space exploration missions. Consequently, to make a choice as objectively as possible, a rigorous method (trade-off analysis) has been used. This analysis is based on the utilisation of a set of Evaluation Criteria (EC), characterised by a "Weight" value (W_v) varying in the range between 1 and 5 and a set of different options. For each EC a Process Criterion Value (PCV) has been assigned. The best choice has been determined by a benefit number (BN), as defined in the following:

Table 1 – Fuel cell classification.

Fuel cell type	Electrolyte	Electrochemical process	
Alkaline Fuel Cell (AFC)	KOH	Anode: $2H_2 + 4OH^- \rightarrow 4H_2O + 4e^-$ Cathode: $O_2 + 4e^- + 2H_2O \rightarrow 4OH^-$ Overall: $2H_2 + O_2 \rightarrow 4H_2O$	
Phosphoric Acid Fuel Cell (PAFC)	H_3PO_4	Anode: $H_2 \rightarrow 2H^+ + 2e^-$ Cathode: $½O_2 + 2e^- + 2H+ \rightarrow H_2O$ Overall: $H_2 + ½O_2 \rightarrow H_2O$	
Proton Electrolyte Fuel Cell (PEFC)	Polymeric membrane	Anode: $H_2 \rightarrow 2H^+ + 2e^-$ Cathode: $½O_2 + 2e^- + 2H^+ \rightarrow H_2O$ Overall: $H_2 + ½O_2 \rightarrow H_2O$	
Direct Methanol Fuel Cell (DMFC)	Polymeric membrane	Anode: $CH_3OH + H_2O \rightarrow 6H^+ + 6e^- + CO_2$ Cathode: $½O_2 + 6e^- + 6H^+ \rightarrow 3H_2O$ Overall:$CH_3OH + ½O_2 \rightarrow 2H_2O + CO_2$	
Molten Carbonate Fuel Cell (MCFC)	Li_2CO_3–K_2CO_3	Anode: $H_2 + CO_3^{2-} \rightarrow H_2O + CO_2 + 2e^-$ Cathode: $½O_2 + CO_2 + 2e^- \rightarrow CO_3^{2-}$ Overall: $H_2 + ½O_2 + CO_2 \rightarrow H_2O + CO_2$	
Solid Oxide Fuel Cell (SOFC)	Solid Oxide	H_2 as fuel: Anode: $2H_2 + 2O^{2-} \rightarrow 2H_2O + 4e^-$ Cathode: $O_2 + 4e^- \rightarrow 2O^{2-}$ Overall: $H_2 + ½O_2 \rightarrow H_2O$	CO as fuel: Anode: $2CO + 2O^{2-} \rightarrow 2CO_2 + 4e^-$ Cathode: $O_2 + 4e^- \rightarrow 2O^{2-}$ Overall: $2CO + O_2 \rightarrow 2CO_2$

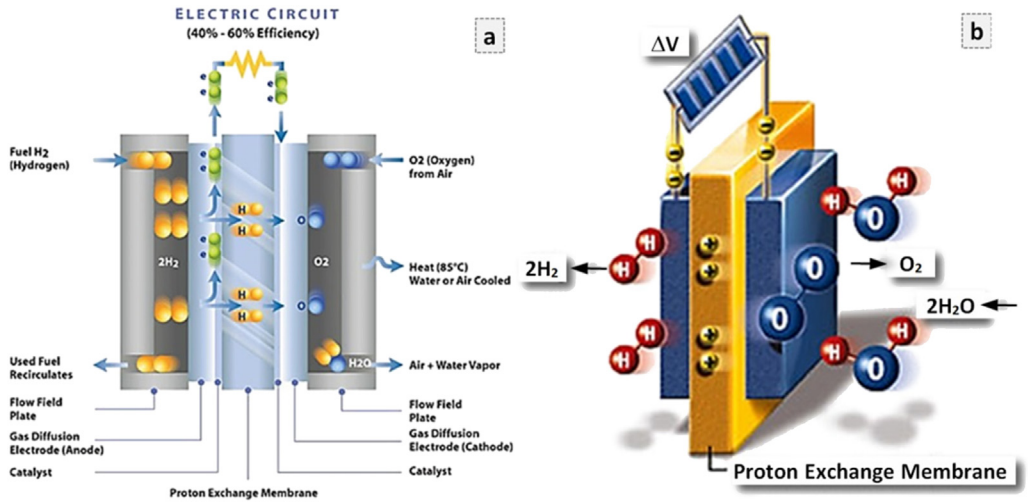

Fig. 1 – Schematic of a FC (a) and of an EZ operation (b).

$$BN = \sum_i PCV_i \times W_i \Big/ \sum_i W_i$$

Fig. 3 schematically represents the method.

In this study, the evaluation criteria have been divided into two main groups: architectural and technological. The "Architectural Evaluation Criteria" (AEC) are a set of characteristics that defines the general aspects of the EPM, the overall mass, the volume, the overall costs. The "Technological Evaluation Criteria" (TEC) are a set of features specifically related to the EPM design (i.e. power density, efficiency, operative temperature). The PCVs have been assigned for each architectural and technological EC dependent on three groups of options: FC Electrolyte options, Regenerative options and Reactant Storage Options. The final selection has been completed by adding the Technological BN (TBN), multiplied for a "k" factor, to the Architectural BN (ABN), and therefore a Final Benefit Number (FBN) has been calculated:

$$FBN = k^*TBN + ABN$$

The "k" factor allows the weight of AEC with respect to TEC to be taken into account. It has been evaluated as the ratio between the maximum scores reached by both the criteria sets.

Table 2 – Fuel cell electrolyser classification.

Electrolyser type	Electrolyte	Electrochemical process
Alkaline	KOH–NaOH	Anode: $2OH^- \rightarrow \frac{1}{2}O_2 + 2e^- + H_2O$ Cathode: $2H_2O + 2e^- \rightarrow H_2 + 2OH^-$ Overall: $H_2O \rightarrow H_2 + \frac{1}{2}O_2$
Proton Electrolyte Membrane (PEM)	Polymeric membrane	Anode: $H_2O \rightarrow 2H^+ + \frac{1}{2}O_2 + 2e^-$ Cathode: $2H^+ + 2e^- \rightarrow H_2$ Overall: $H_2O \rightarrow H_2 + \frac{1}{2}O_2$
Solid Oxide (SOFC)	Solid Oxide	Anode: $2H_2O + 2e^- \rightarrow 2O^{2-} + 2H_2$ Cathode: $2O^{2-} \rightarrow O_2 + 2e^-$ Overall: $H_2O \rightarrow H_2 + \frac{1}{2}O_2$

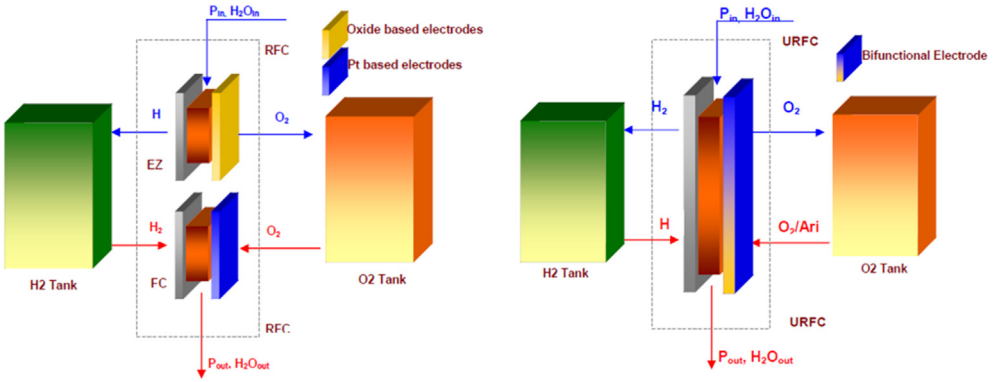

Fig. 2 – Schematic of a RFC and URFC architectures.

Table 3 – Hydrogen storage methods.

Storage method	Mass (kg H_2/system mass %)	Temperature (°C)	Pressure (bar)	Phenomena and remarks
High pressure gas cylinder	8–12	Room	800	Compressed gas in lightweight gas cylinder.
Storage as cryogenic liquid	15–40	−253.15/−243.15	1–8	Liquid Hydrogen – continuous loss of a few % per day of H_2 at room temperature.
Storage as a dense gas at reduced temperature	10–20	−180.15/−153.15	350–500	Dense gas at supercritical pressure
Storage as adsorbed hydrogen on a sorbent	10	−80	100	Physiosorption on materials with a very large specific surface area.
Storage on nanocarbon	6–50 (theoretical)	−196.50/24.85	0.4–120	Storage on defective structures of carbon nanotubes
Storage in metal hydrides	5–7	Room	1	Hydrogen intercalation in host metals, metallic hydrides.

AEC and TEC are listed in Table 4 with the W_u and its justification:

Trade-off results

FC electrolyte options

In Table 5 the FC Electrolyte Options are summarised, reporting their main advantages and drawbacks:

Table 6 reports the estimated Architectural and Technological PCVs for each FC Electrolyte Option. As can be seen, the PEFC comes out as the best candidate in terms of architectural and technological point of view.

The FBNs, obtained as explained in Section 3.1.1, give the same result (Table 7).

Regenerative options

The Trade-Off of Regenerative Options has been performed comparing a typical complete space system composed of an FC, EZ (if present), Storage and ancillaries. The FC Regenerative Options are summarized in Table 8, reporting their main advantages and drawbacks:

Using the same procedure applied for FC electrolyte options, the FBNs listed in Table 9 have been obtained.

As can be noticed the Discrete RFC with PEM EZ results as the best choice. Regarding the effect of stack pressure, operation at pressures higher than the ambient has been considered. In fact, increasing the operative pressure leads to a better fuel cell performance and efficiency, especially if pure hydrogen and oxygen are used. For space application, due to the availability of pressurized hydrogen and oxygen, there are no penalty in the balance of plant for the pressurization. In this regard, operation of the hydrogen/oxygen fuel cell at high pressure is preferable.

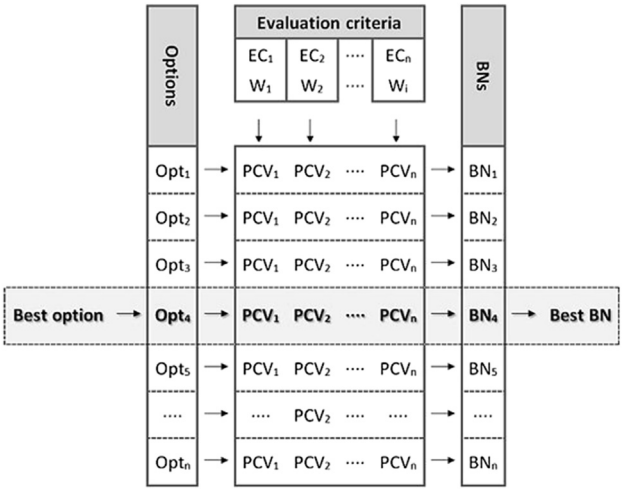

Fig. 3 – Trade-off method schema.

Reactants storage options

The Reactants Storage Options are listed in Table 10 in terms of advantages and drawbacks.

Table 11 lists the obtained FBNs, as can be seen, the high pressure gas cylinder is the best choice. This result derived from several considerations involving: the technologic readiness level (such technology is well known and mature), the lifetime (up to 20,000 cycle have been proved), the overall cost (minimal balance of plant is required). Even the high storage pressure implies some safety issues to be considered, risks for humans can be minimized due to the high maturity level of the technology. The storage of hydrogen as cryogenic liquid or dense gas, is very promising from the energy density point of view, but the use of cryo-tanks dramatically increases the system complexity.

Fuel cell technology selection

The performed Trade-Off analysis has resulted in the following architectural choices:

- Discrete RFC System;
- PEM - based FC;
- PEM- based EZ;
- High pressure gas cylinder Hydrogen/Oxygen storage;

A regenerative system is necessary to exploit the surplus of power coming from a primary source (i.e. solar arrays) [22]. Regenerating the FC reactants (Hydrogen and Oxygen) implies a significant reduction of the overall system mass. Having a discrete RFC (FC + EZ) allows high round-trip efficiencies and auxiliaries sharing. PEM based FCs allow compact, robust and simple mechanical design, relatively long operating life, quick start-up, low temperature and pressure, high voltage and power density operation, good efficiency (50%), handling, assembly and tightness less complex than other types of fuel

Table 4 – Architectural and technological evaluation criteria, description and weights.

Criterion name	Criterion relevance assessment	W_v
Architectural evaluation criteria		
EPM system overall mass	A low overall mass is preferable to reduce costs, due to the impact on transportation and delivery systems. A heavy system could make the mission unfeasible.	5
Logistic mass rate	A high Logistic Mass Rate could make the mission unfeasible for programmatic and economic issues.	5
EPM system envelope/volume	The EPM system volume and envelope have to be compatible with the maximum volume/envelope available within the lander. A limited volume allows for a larger number of transportation possibilities, reducing the impact onto the transportation segment.	3
Synergies with other architecture elements and/or subsystems	More integrated, redundant and efficient architectures can be obtained sharing some functionalities between the EPM system and other subsystems. Technological synergies lead to less expensive and risky development and to important mass savings, but does not impacts on the mission feasibility.	3
Growth capability	Represents the possibility of the EPM system to be easily expanded for providing higher levels of power and energy for future Space Exploration Missions on Lunar Surface, without the need for completely new/different elements to be developed and deployed on the Moon. In fact, future missions are expected to be more power demanding, thus it is of primarily importance to limit the resources required to sustain these missions.	4
Required maintenance	The higher the required maintenance time the lower the operative time. EPMs requiring the lowest amount of maintenance are preferred. This aspect have an impact on the mission feasibility.	4
Risk for human	As for any other spacecraft interacting with the astronauts, the safety of human have the highest priority.	5
Technology Readiness Level (TRL) and technical risk	A higher TRL means that the considered technology have reached a high level of maturity and, then, requires lower costs (and time) for the next developments until to be ready to flight.	2
Lifetime	Lifetime, and related degradation in performances, is a key factor to limit maintenance missions and to get a feasible overall mission.	5
Overall costs	To get the required financial support the Life Cycle Cost represents an important factor for a mission.	3
Support services	EPM systems generally have several dependences from services of other subsystems, some of which have a major impact onto the whole element architecture, e.g. the thermal control.	4
Energy storage range	Because the EPM system has to provide power to the other Elements/ Subsystems, greater the range of energy storage reachable with the selected technology, greater the possibility to use it. This range is a driving factor for the feasibility of the mission.	4
Power range	Because the EPM system has to provide power to the other Elements/ Subsystems, greater the range of power reachable with the selected technology, greater the possibility to use it. This range is a driving factor for the feasibility of the mission.	4
EPM commonalities for different applications	A common development reduces the development efforts, this criterion is of major relevance.	4
Technological evaluation criteria		
Implementation issues	The implementation issues have an important impact on the feasibility on lunar surface of the FC process.	5
Scalability	The possibility to scale-up the FC can be demonstrated by a smaller plant than the one required to meet the power production requests, reducing its implementation and mission costs. This aspect does not impacts directly on the system feasibility, but only on its implementation.	3
Availability of terrestrial counterparts	The considered FC technologies have already been developed for ground application, the terrestrial availability counterparts is generally high.	2
Inherent safety	Safety aspects are of primary importance for use of FC in Human Exploration missions.	5
Complexity and reliability	This criterion concerns the number of subsystem and ancillaries A reduced number of ancillaries lead to a more efficient and reliable EPM system.	4
Robustness w.r.t. the Moon and space environments	The system is not directly exposed to the moon or space.	4

Table 4 – (continued)

Criterion name	Criterion relevance assessment	W_v
Operative temperature and heat	This criterion concern the adaptability of the system with respect to the temperature, the higher the temperature range the lower the thermal conditioning system requirements. Because the system has to be packaged and thermally conditioned, a higher operative temperature implies a low heat exchangers surface and thinner insulations. Due to the large amount of power required for PLR and LB operation, the FC produce a large amount of thermal power to be managed, this issue strong impact the overall system design.	5
Efficiency	A higher EPM system efficiency implies a lower reactants consumption. This efficiency is related to the chemical process capability to extract the energy from the used reactants, and depend by the adopted fuel cell technology.	5
Power density	High power density lead to a lighter and smaller system.	5
Start-up required time	A fast start – up time of the EPM system is fundamental to reduce delay after switching on.	5
Energy density	A high specific energy density implies a low reactants storage volume.	5
Internal parasitic energy & power	Subsystems and components are necessary to run the EPM system. The lower internal parasitic energy the higher the net efficiency of the system.	4
Modularity	The possibility of the EPM system to have a modular design, in order to be able to be implemented in different configurations, based on a single common architecture, capable to afford different energy and power demands. As it is explicitly required by ESA, this criterion is of major relevance.	4

cells. Moreover, the solid, polymeric, non-corrosive electrolyte, increases the operational safety and eliminates the issues related to the handling and resupply of liquids. The PEM based EZs are extremely compact, due to the high current density operation, with a conversion efficiencies ranging from 50 to 90%. As the PEFC, the PEM EZs are safe and reliable because they use a solid, polymeric electrolyte, they operate at a high current density, and have the intrinsic ability to cope with transient variations in electrical power input. Due to the well-established technology, the compressed gases can be stored at high pressure within lightweight tanks with a high degree of reliability.

The EPM systems design and requirement analysis

Overview of studied applications

The context and the requirements of the EPM system, based on Fuel Cell technology, have been defined considering as reference the last studies on the possible lunar architectures for the future human space exploration of the Moon, carried out in Europe and by the International Space Exploration Co-ordination Group (ISECG, [23]). Fuel Cell technology has been considered as suitable for a Lunar Power Plant (LPP) and a Pressurized Lunar Rover (PLR). Even if the two applications are completely different, the EPM systems that power them have common requirements: solar powered, high power peaks to be covered, high levels of energy to be provided, reliability and robustness, that guarantees the human crews safety and limits the mass to be deployed on the Moon surface. Therefore, an EPM system based on common architecture and technology has been envisaged [24]. Fig. 4 shows an artistic concept of power plant and lunar rover.

Lunar power plant sizing

The lunar power plant has been conceived as reusable and relocatable several times and can be placed at equatorial and polar latitudes of the moon. The LPP concept is based on a set

Table 5 – FC electrolyte options – advantages and drawbacks summary.

Electrolyte options	Advantages	Drawbacks
AFC	Low manufacturing and operation costs, heavy compressor not needed, fast cathode kinetics	Large size, pure H_2 and O_2, corrosive liquid electrolyte.
PAFC	Commercially available, lenient to fuels, heat for cogeneration	Low efficiency, limited service life, expensive catalyst
PEFC	Compact design; long operating life, quick start-up, low temperature operation, operates at 50% efficiency	High manufacturing costs, pure hydrogen, auxiliary equipment for heat and water management
DMFC	Compact design, no humidification needed; liquid feed	Complex stack structure, slow load response
MCFC	Highly efficient, utilizes heat for co-generation.	Electrolyte instability, limited service life
SOFC	High efficiency, lenient to fuels, natural gas directly, no reformer	High operating temperature, exotic metals, high manufacturing costs, oxidation issues, low specific power

Table 6 – FC electrolyte options – architectural and technological benefit number.

Architectural PCV

FC electrolyte option	EPM system overall mass	Logistic mass rate	EPM system envelope/ volume	Synergies with other architecture elements and/ or subsystems	Growth capability	Required maintenance	Risk for human	TRL and technical risk	Lifetime	Overall costs	Support services	Energy storage range	Power range	EPM commonalities for different applications	Architectural benefit number
AFC	2	1	4	4	4	4	3	5	1	4	3	N/A	2	5	3.0
PAFC	2	5	2	5	4	4	3	2	5	4	3	N/A	1	5	3.5
PEFC	5	4	5	5	4	4	4	4	4	3	5	N/A	5	5	4.4
DMFC	3	2	3	2	4	4	5	2	2	3	5	N/A	1	3	3.1
MCFC	3	2	1	2	4	3	1	2	2	2	3	N/A	5	3	2.6
SOFC	1	4	1	2	4	3	2	2	2	2	3	N/A	5	3	2.7

Technological PCV

	Implementation issues	Scalability	Availability of terrestrial counterparts	Inherent safety	Complexity and reliability	Robustness w.r.t. the moon and space environments	Operative temperature and heat	Efficiency	Power density	Start-up required time	Energy density	Internal parasitic energy & power	Modularity	Technological benefit number
AFC	4	5	5	3	4	3	4	4	4	5	N/A	5	5	4.2
PAFC	4	5	5	3	4	3	3	3	3	5	N/A	5	5	3.9
PEFC	5	5	5	4	5	3	5	4	5	5	N/A	5	5	4.6
DMFC	4	5	5	4	4	3	4	3	4	5	N/A	5	5	4.2
MCFC	2	5	5	1	2	3	2	5	1	2	N/A	5	5	2.9
SOFC	3	5	5	2	2	4	2	5	3	2	N/A	5	5	3.4

Table 7 – FC electrolyte options – final benefit numbers.

FC electrolyte option	ABN	"K" factor	TBN	FBN
AFC	3.0	1	4.2	7.2
PAFC	3.5	1	3.9	7.4
PEFC	4.4	1	4.6	9.0
DMFC	3.1	1	4.2	7.2
MCFC	2.6	1	2.9	5.5
SOFC	2.7	1	3.4	6.1

of identical Lunar Power Plant Elements (LPPE) linked together. During the daylight each LPPE provides power and stores energy using the solar array panels and EZ, during the night using the FC. In case of short term power peaks the FC operates at higher specific current densities, to satisfy the power demand (up to 400% more than the nominal level). This assumption even if is uncommon for terrestrial fuel cells operated with air, where a power capability (peak power/nominal power) of 1.5–2.0 is normal, can be acceptable for pure oxygen systems. In fact, due to the use of pure oxidant, the performance of the fuel cell are considerably enhanced, leading to a fuel cell power capability of more 6 in some cases. Concerning the durability of the fuel cell stack, the fuel cell degradation is primarily related to the potential window that is smaller at high current than at low current. Thus peak power is less critical in terms of cathode degradation than at lower power levels. Each LPPE is connectable with other LPPEs and other elements. The configuration of each LPPE has been conducted considering the compatibility with the space transportation system (confined cylindrical volume of 3 m of diameter), easy accessibility for critical components maintenance and substitution and to the external power interfaces. An octagonal shape, with a diameter of 3.0 m and height of about 2.5 m, (in stowed configuration) has been adopted. To obtain a symmetrical mass distribution and a short path to the radiators, all the main, critical, LPPE components (FCs, EZ, Batteries, Power Control and Distribution Unit (PDCU), Command and Data Handling (C&DH) Transponders, and water and oxygen tanks are hosted in a chest on top of the tower, with a truncated octagonal shape of 0.5 m in height. The room for the hydrogen tank has been placed at the bottom of the LPPE and mounted on top of an adapter ring, for lander and transport elements connection. Up to four energy expansion units of 660 kWh each, consisting of additional tanks of H_2, O_2 and water can be installed on the chest (water and O_2 tanks) and onto the tower (H_2 tanks), increasing the capability of energy storage of the system. The deployable bi-axial solar trackers and radiators are placed on top of the chest, to allow the maximum solar radiation to be exploited and the exposure to the cold sky of the Moon. A four legged system sustains the

Table 9 – Regenerative options – final benefit numbers.

Regenerative option	ABN	"k" factor	TBN	FBN
URFC	3.4	1.02	4.3	7.8
Discrete RFC with Alkaline EZ	3.7	1.02	3.9	7.6
Discrete RFC with PEM EZ	4.4	1.02	4.5	9.1

LPPE and hosts the external interfaces. Fig. 5 shows the external and internal configurations of the LPPE with the following specifications:

- Solar Arrays: 5 panels, total area 27 m^2, total max power 6.5 kW;
- Fuel Cell: 2 modules, nominal power 4.3 kW;
- High pressure Electrolyzer (350 bar): 2 modules, nominal required power 645 W;
- Tanks: 11 spherical tanks for H_2, O_2 and H_2O, stored energy 320 kWh;
- Battery: 3 modules for start-up in shadowed area only;
- Power Conditioning and Distribution Unit: three voltage power delivery buses 28, 120, 360 V;
- Energy Expansion Modules: additional store of 660 kWh;
- Interfaces and Distribution System: including a 3 m robotic arm and 30 m cable, 6 plugs;

The total mass budget of the LPPE has been estimated in 982 kg that is compatible with the conceived space transportation system. The study has been focused on different power plant architectures: 1) the equatorial and polar architecture, composed of two PLRs, assuring long range mobility capability, two robotic mobility systems (large and medium) aimed at transporting payloads over variable distance and one unpressurized servicing rover, a medium habitat module sustaining 4 astronauts for medium duration missions (14–28 days), a fixed power plant that continuously supports the habitat module and recharges the mobile elements; 2) the Polar Outpost, which consists of a fixed large settlement composed by the same unpressurized and pressurized vehicles considered for the equatorial and polar architectures, a large habitat module for long duration missions (70–180 days), a fixed power plant and an In Situ Resources Utilization (ISRU) plant for the exploitation of the in – situ resources for life supporting (i.e. oxygen or water production). Due to different locations (equatorial or polar latitude) and architectures, the energy demands are covered by a combination of a different number of LPPEs. Table 12 lists the energy demands, and the envisaged LPP configurations:

As can be noticed in Table 12, although the same architecture and power needs exist for the equatorial and polar

Table 8 – Regenerative options – advantages and drawbacks.

Regenerative option	Advantages	Drawbacks
URFC	Light system due to unified FC-EZ Reduced system complexity because auxiliary sharing	FC and EZ power are linked Bifunctional electrode not already optimised
RFC with Alkaline EZ	No constrains in FC and EZ power well established technology for Alkaline EZ	Heavier system due to discrete arrangement Corrosive electrolyte
RFC with PEM EZ	FC and EZ high efficiency, no corrosive electrolyte, same FC and EZ technology possible auxiliaries sharing	Heavier system due to discrete arrangement

Table 10 – Reactants storage options – advantages and drawbacks.

Storage options	Advantages	Drawbacks
High pressure gas cylinders	Compressed gas in lightweight cylinder.	High cost of encapsulation materials
Cryogenic liquid	High H_2 storage capacity (gravimetric)	Continuous loss (few% per day) of H_2 at RT. Complex system
Dense gas at reduced temperature	Increased storage w.r.t. high pressure cylinder	High cost of encapsulation. Low temperatures (80 K)
Adsorbed hydrogen on a sorbent	High pressure H_2 stored in low pressure tank	Process requires thermal energy
Nano carbon	Potentially high storage capacity	Technology at basic research level
Metal hydrides	High volumetric storage capacity.	Heavy materials. Process requires thermal energy

Table 11 – Reactants storage options – final benefit numbers.

Reactants storage option	ABN	"k" factor	TBN	FBN
High pressure gas cylinder	4.3	0.98	4.1	8.3
Storage as cryogenic liquid	3.6	0.98	3.2	6.8
Storage as a dense gas at reduced temperature	3.8	0.98	3.5	7.3
Storage as adsorbed hydrogen on a sorbent	3.1	0.98	3.5	6.6
Storage on nano carbon	3.1	0.98	3.3	6.3
Storage in metal hydrides	3.6	0.98	3.6	7.1

installations, the different duration of lunar night (120 h/month for polar site, 336 h/month for equatorial site) implies a higher night maximum energy demand for the equatorial architecture. The polar outpost, because of the larger dimension of the settlement and the possibility of long duration missions, features the maximum power and energy requests.

Pressurized lunar rover sizing

The PLR has been designed considering five different power profiles, based on a 24 h day: T1, (Manned Travelling Day, during daylight), T2 (Manned Travelling Day, during night and contingency), E1 (Extra, Vehicular Activity (EVA) dedicated Day, during daylight), U1 (Unmanned Travelling Day), C1 (Emergency day). Fig. 6 depicts the power demands that have been considered for each power profile, over 24 h.

T1 and T2 power profiles, include 10 h of PLR movement, with periods of power peaks due to harsh terrains or steep slopes. T1 and T2 profiles have the same power budget, the only difference is that T2 operation is concerning the power delivery during lunar night or shadowed areas. The E1 power profile is representative of the PLR in a static position during crew excursion outside the PLR that has to be foreseen only during the daylight. The U1 profile is representative of the PLR power demand during unmanned travelling for 10 h a day. The C1 is representative of the PLR power demand

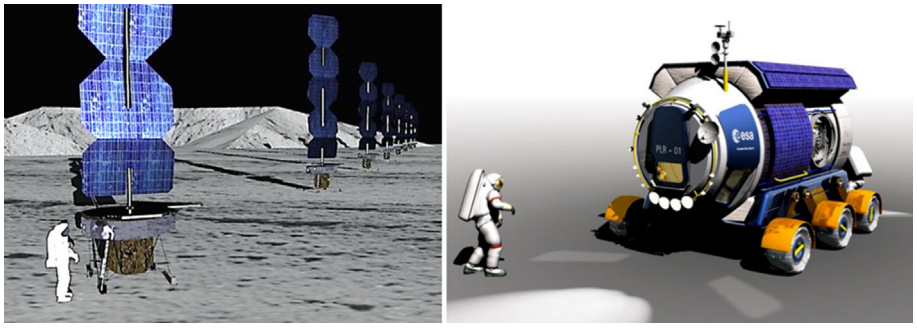

Fig. 4 – LPP (source: CGS/ESA) and PLR artistic concepts (source: TAS-I/ESA).

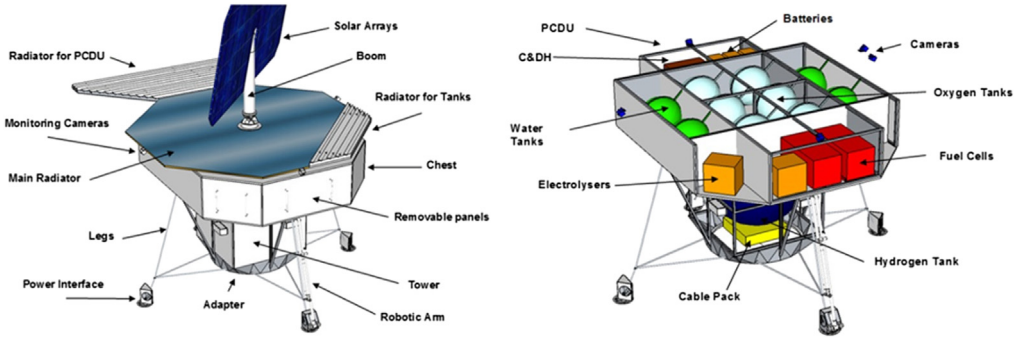

Fig. 5 – LPPE architecture concept (source: CGS/ESA).

Table 12 – LPPs energy demands and configurations as function of different architectures.

Architecture	Day max power [kW]	Night max power [kW]	Night max energy [kWh]	Human	Number of LPPE	Energy expansion unit
Equatorial architecture	10.80	9.70	3257	Yes	2	4
Polar architecture	10.80	9.70	1163	Yes	2	1
Polar outpost	106.70	51.10	6137	Yes	25	4

needed in case of a serious contingency, when it is impossible to take the astronauts back to the lunar base. In this situation the PLR is idle, operated at a low power consumption mode and used as safe haven for supporting the crew up to the arrival of the rescue mission (for a maximum 15 days). Table 13 summarizes the maximum continuous power and energy demands and peaks, of the described power profiles.

As can be noticed, the FC produces the higher power levels and the maximum continuous power in correspondence of T2 power profile. Thus, the power of FC stack has been sized to cover this power request (8.40 kW of maximum continuous power and 12.80 kW of peak power). The power profiles can be combined to derive different operative plans. All the operative plans include two T2 days, added at the end of the 14 days of nominal mission, extending the single excursion of the PLR (to afford any contingencies that could delay the vehicle return to the base) to a maximum of 16 days. The maximum energy produced by EPM system, that has been calculated in case of contingency, is 220 kWh. Such amount of energy corresponds to the energy consumption during two consecutive T2 days and it is supposed to be delivered by the FC stack only. Table 14 lists some examples of operative plans performed by PLR during a typical manned mission.

PLR and LPPE EPM system architecture

A similar architecture of the EPM system has been foreseen for both the applications. It is based on a common configuration: 2 power sources (solar arrays and RFC), 2 storage devices (RFC and Batteries), 1 Power Conversion and Distribution Unit (PCDU), several internal and external power connections. The power management is performed through a combination of Solar Arrays and RFC (operating in FC mode) on the basis of the On Board Data Handling (OBDH) requests. During the lunar daylight the Solar Arrays cover the power demand and supply the EZ for Fuel Cell reactants regeneration by means of an Array Power Regulator (APR), whereas the FC stack covers the peak power. During the lunar night the power requirement is satisfied entirely by the

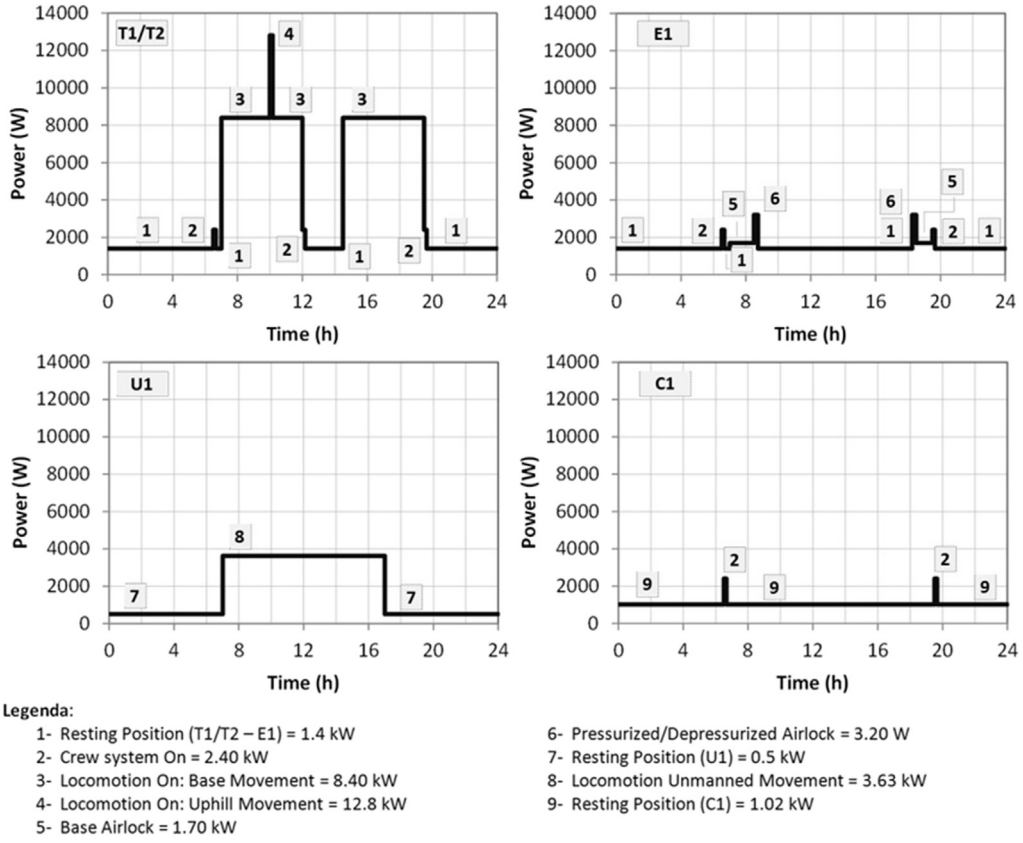

Fig. 6 – Considered power profiles for PLR EPM system sizing.

Table 13 – PLR energy and power requirements.

Power profile	Max continuous power [kW]	Peak power [kW]	Total energy request [kWh]	Continuous power (Device)	Peak power (Device)
T1	8.40	12.80	104.83	SA + FC	FC + BAT
T2	8.40	12.80	104.83	FC	FC
E1	1.70	3.20	35.58	SA	SA
U1	3.63	–	43.25	SA + FC	FC/BAT
C1	1.02	2.40	24.94	SA	SA

RFC (operating in FC mode). An auxiliary battery stack assures the RFC start up in shadowed areas and during the lunar night. The Power Conditioning Block manages the energy sources to obtain a 120 V regulated main bus and supply the Power Distribution Units (PDU) and the PCDU. RFC and batteries are connected to the 120 V bus via an FCCR (Fuel Cell Charge Regulator) and a BCR (Battery Charge Regulator) in case of power charge. In case of power production an FCDR and a BDR (Fuel Cell Discharge Regulator and Battery Discharge Regulator) are used for power conditioning. Besides the 120 V distribution, it has been foreseen to provide several 28 V power lines for the lower power loads, by means of a dedicated Low Power Distribution Unit (LPDU). In the case of LPPE, a third high voltage bus (360 V, High Power Distribution Unit, HPDU) has been included, to allow the power to be transported over longer distances (up to 300 m). The overall control of the system (monitoring, redundancy management and regulation) is performed by additional electronics like a reliable Main Error Amplifier (MEA), a distributed bank of self-healing and high frequency ceramic capacitors, and a TMTC (TeleMetry and TeleCommand) unit. Fig. 7(a) shows the EPM system architecture for the PLR application. The LPPE architecture is similar, the main differences are related to the distribution/interfaces and to the additional energy storage units, (Fig. 7(b)).

The fuel cell breadboard

To demonstrate the technology chosen for the PLR and LB EPM systems, a FC breadboard has been designed, manufactured, assembled and tested. In this way the behaviour and the feasibility of the PEM - based RFC system has been evaluated. Considering the nominal power to be produced (4.9 kW for LPPE, 8.4 kW for PLR with a peak power of 12.8 kW) by the FC stack and the maximum energy to be stored (320 kWh for LPPE, 220 kWh for PLR), the size of the FC stack has been calculated minimizing the overall system mass composed by: FC stack, tanks, Electrolyser and Pipes/Harness [25,26]. In a typical polarisation curve the fuel cell voltage decreases with the current density. This implies that the efficiency decreases by increasing fuel cell power density, thus the fuel cell stack mass is in inverse proportion with the fuel cell efficiency. On the contrary, a decrease in efficiency, considering the net energy to be produced as a constant, leads to a higher fuel quantity to be stored, thus the tank mass is in direct proportion with the efficiency. Moreover, the higher the efficiency the lower the waste heat to be dissipated becomes. Considering the electrical efficiency, it can be calculated as follows:

$\eta = 0.675V_c$, where V_c is the stack the cell voltage

As stated above, the overall mass of the system can be estimated as:

$$m_{sys} = m_{FC} + m_{TA} = \eta k_{FC} + \eta^{-1} k_{TA}$$

where : m_{sys} = system mass; m_{FC} = FC mass; m_{TA} = Tank mass

the k_{FC} and k_{TA} are constants that take into account some design parameters such as the materials, the geometry of tanks (spherical or cylindrical) and the stack design factor (kg/m^2 of active area). On the basis of these considerations, two different optimal current density has been calculated for LPPE and PLR stacks, they share the same bipolar plate design with different number of cells (Table 15).

The fuel cell stack developed for the breadboarding activity, has been designed and manufactured accordingly to the background experience at CNR-ITAE [27–30]. It is composed of two modules of ten cells each, with a total nominal power of 1.00 kW at 80 A and 14.6 V. Each module represents a sub - unit of the stack designed for the LPPE and PLR, thus it has the same bipolar plate configuration with a different cell number. The overall dimension of the device resulted in 14.6 × 26.9 × 11.4 cm with the two stacks electrically connected in series. Three different configurations for the breadboard have been conceived: i) Basic (BBB), composed of the developed Fuel Cell Stacks connected to the test station; ii) Stand - Alone (BSA), consisting of an integrated self-stand unit composed of the fuel cell stacks, the reactant supply subsystem, the electrical control subsystem and the data acquisition

Table 14 – Examples of PLR operative plans.

Operative plane opt.1	T1	E1	T1	E1	T1	E1	T1	T1	E1	T1	E1	T1	E1	T1	T2	T2
Operative plane opt.2	T1	T1	E1	T1	E1	T1	E1	T1	E1	T1	E1	T1	E1	T1	T2	T2
Operative plane opt.3	T1	T1	T1	E1	E1	T1	E1	E1	T1	E1	T1	E1	T1	T1	T2	T2
Operative plane opt.4	T1	T1	E1	T1	T1	E1	E1	T1	E1	E1	T1	T1	E1	T1	T2	T2
Day	1	2	3	4	5	6	7	8	9	10	11	12	13	14	15	16
	16 days mission = 14 days + 2 day (contingency)															

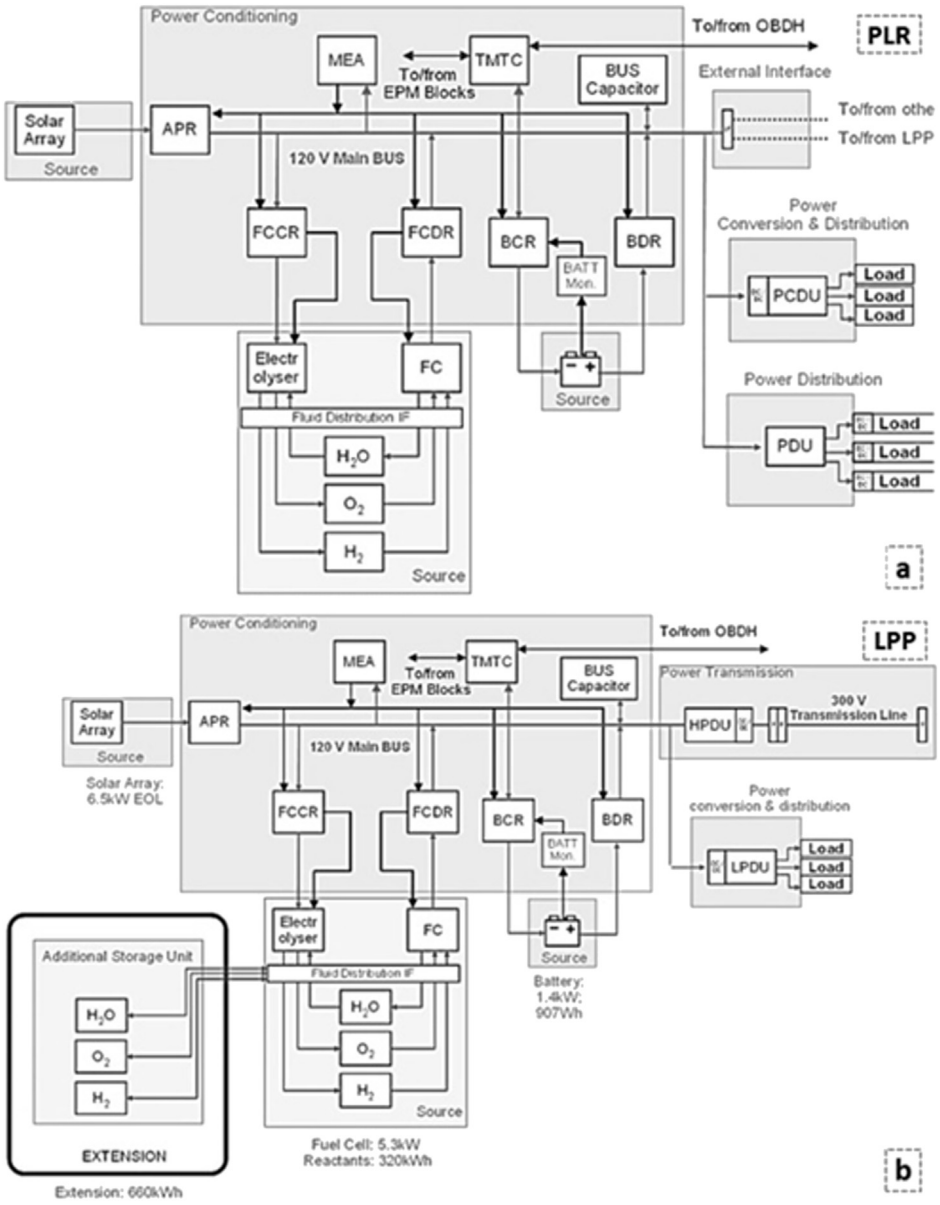

Fig. 7 – PLR EPM system architecture (a), LPPE EPM system architecture (b).

unit; iii) Closed-Loop (BCL), consisting of the stand-alone breadboard connected to a commercial EZ. The BBB has been used to completely characterize the fuel cell stacks. The influence on the FC stack performance in stand alone configuration due to the integration process has been evaluated, and the BCL has been used to demonstrate the RFC EPM system feasibility. Fig. 8 shows the two manufactured stacks and the three breadboards:

Table 15 – LPPE and PLR stack characteristics.

	LPPE	PLR
Stack number	2–75 cells each	2–82 cells each
Active area	160 cm^2	160 cm^2
Current density	300 mA/cm^2	500 mA/cm^2 (nominal)–900 mA/cm^2 (peak)
Stack voltage and current	55.4 V–48 A	55.4 V–80 A (nominal) – 46.5 V–144 A (peak)
Stack efficiency	54%	49% (nominal) 41% (peak)
Stack nominal power	2661 W	4432 W (nominal) - 6692 W (peak)
Operative temperature	75 °C	75 °C
Operative pressure	3 bar_{abs}	3 bar_{abs}
Total EPM system mass budget	591.60 kg	480.00 kg

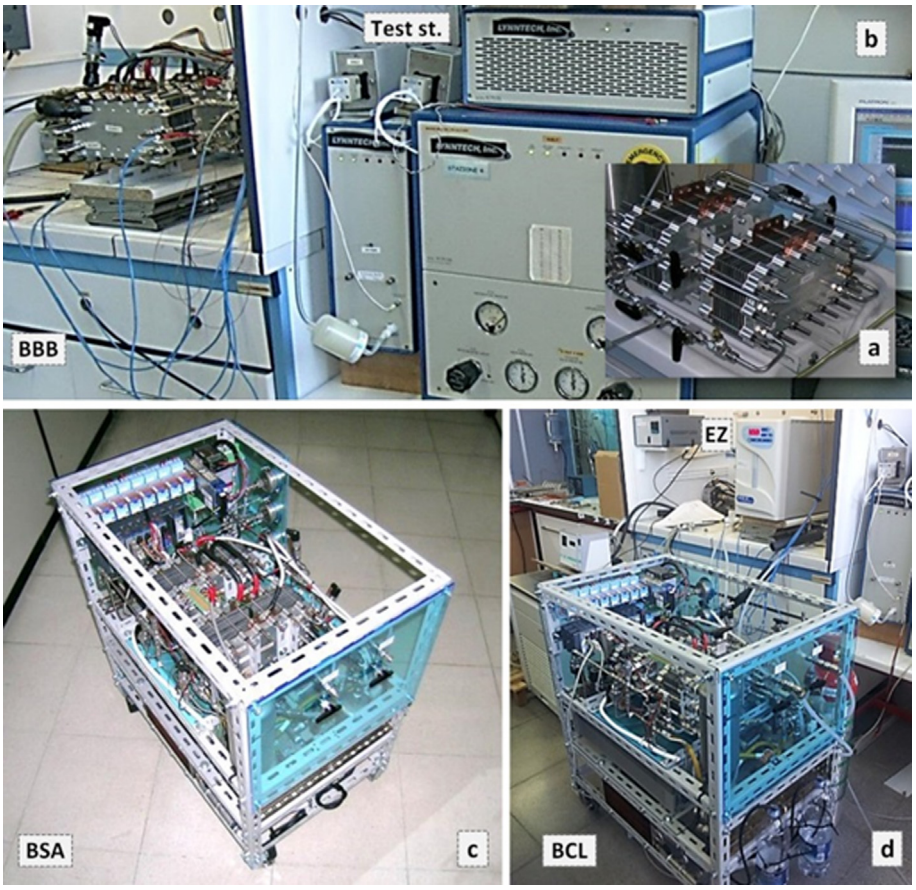

Fig. 8 – a) Assembled stacks, b) BBB, c) BSA; d) BCL.

Test plan

A complete set of preliminary checks have been performed after the FC stack assembly, to verify the electrical insulation of the components, the external leakage and the internal fluids crossover. A conditioning phase has been carried out after each assembly of the fuel cell stacks, to correctly activate the MEA catalyst and membrane, and, consequently, to reach higher MEA performances. The conditioning, made only on BBB configuration, has been performed by warming up the stack to a temperature of 80 °C and then providing fully humidified reactants. A constant voltage of 0.6 V per cell has been applied and the current has been monitored until stabilization. A constant value of current has been recorded after about 8 h. Successively, to point out the fuel cell stack performance, a set of three *I*–*V* curves has been recorded (H_2/Air, T = 80 °C, 3 bar_{abs} H_2/Air stoichiometry = 1.5/2.0, H_2/Air RH % = 100/100) by changing the current density and recording the correspondent voltage. Each current step has been maintained for at least 10 min, until voltage stabilization, and the voltage recorded as the mean of the last minute. The average of these three curves has been considered as the baseline for the successive tests. Once the MEA has been conditioned, a set of *I*–*V* curves have been generated considering operation conditions representing the running integrated system (H_2/O_2, T = 75 °C p = 3 bar_{abs}, H_2/O_2 stoichiometry = 1.5/2.0H_2/O_2 RH % = 50/50). This test has been carried out only on BBB configuration. A stationary state test (time test), where a specific current point is set for pre-determined operating conditions and the voltage is recorded has been run. It is performed to identify the fuel cell behaviour when a steady load is applied. This test points out the breadboard voltage stability at the design current density. It has been performed on BBB (in the same *I*–*V* operative conditions) and in BSA configurations (H_2/O_2 T = 75 °C p = 3 bar_{abs}, H_2/O_2 stoichiometry = recirculated H_2/O_2 RH% = recirculated). To evaluate the gravity effects on the electrochemical reactions [31,32], inclined plane tests have been performed. Indeed, a PEM fuel cell produces water at the cathode surface that, in a conventional configuration, is parallel to the plane of bipolar plate channels. Thus, the water moves towards the channels through the GDL, perpendicularly to the gravity vector. The water motion can be influenced depending on the orientation of the bipolar plate with respect to the gravity. A sequence of *I*–*V* curve and time test has been performed only on the BBB, considering four different inclinations of the FC stack, as Fig. 9 depicts:

To evaluate the power response of the BBB, when a cyclic load profile is applied, a 14-days Load Cycles, has been conceived. Particularly, a power load representative of T1 and T2 power profile (see Fig. 7) has been designed of the reference operational power profile provided by ESA [1]. The 14 nominal days are represented by 7 real days of test lasting 8 h, moreover, the T1 power profile has been modified to represents

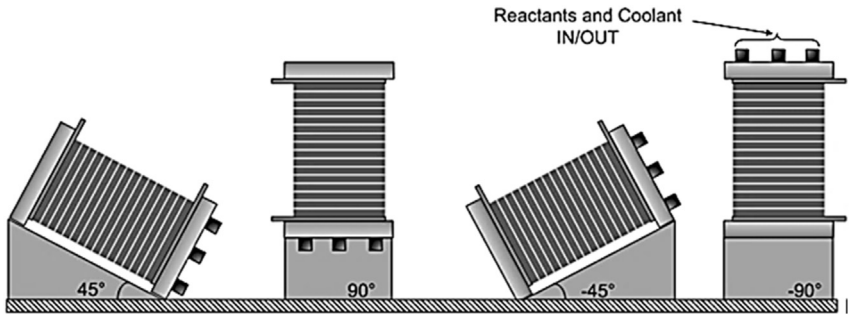

Fig. 9 – Stack attitudes for inclined-plane tests.

different types of missions. In particular three profiles have been defined; $T1_{FC}$ (nominal power profile), TL_{FC} (long duration power profile) and TV_{FC} (quick variation power profile). The used power profiles are represented in Fig. 10:

The corresponding power levels are listed in Table 16:

Table 17 summarises the power profile combinations used to obtain three different operative plans, performed during 9 days (7 + 2 contingency days). As can be seen, all the cycles have been concluded with the power profile representative of the 2 contingency days ($T2_{FC}$).

To demonstrate the breadboard functioning in a quasi-closed-loop operational mode, a commercial hydrogen generator has been used together with the breadboard to regenerate hydrogen from the water produced by the stack during its operation (EZ mode). Each cycle takes about 3.5 h for charging H_2 tank (10 L at 14 bar) and about 15 min for tank discharge and test. The regenerated reactant has been used to feed the Fuel Cell and this cycle has been performed ten times. This test has been performed only on BCL configuration.

Test results

Test on BBB configuration

Conditioning tests have been carried out with fully hydrated hydrogen and air. This test allowed the MEAs to be broken – in and provided the baseline for the successive tests. After the steady conditioning test (H_2/Air, T = 80 °C, 3 bar_{abs} H_2/Air stoichiometry = 1.5/2.0, H_2/Air RH% = 100/100), the polarisation curve of the FC stack has been defined. As described in the above section, Fig. 11 shows the average of the three performed I–V curves, in comparison with that carried out with pure hydrogen and oxygen.

Operating the stack with fully humidified hydrogen and air, a power of 1178 W has been achieved at 500 mA/cm^2, with a voltage of 14.72 V, whereas at 1000 mA/cm^2 a power 1984 W has been recorded. In case of pure oxygen the overall performance, were almost unchanged up to 800 mA/cm^2. From here on out the two curves begin to diverge. This behaviour is mainly due to the lower reactants humidification affecting the proton conductivity of the membrane and mitigating the positive effect of pure oxygen. However at higher current density, where a higher mass transfer rate is required, using oxygen instead of air always enhanced the FC stack performance. In this case, a power of 1173 W has been achieved at 500 mA/cm^2, with a voltage of 14.66 V. The highest power of 2086 W has been reached at 1000 mA/cm^2 with a voltage of 13.04 V.

The time test confirmed the performances obtained with the I–V curve. Indeed, under a constant load of 80 A (500 mA/cm^2) an average voltage of 14.61 V has been recorded that corresponds to a power of 1174 W (Fig. 12), with a voltage decay of 99.45 mV/h.

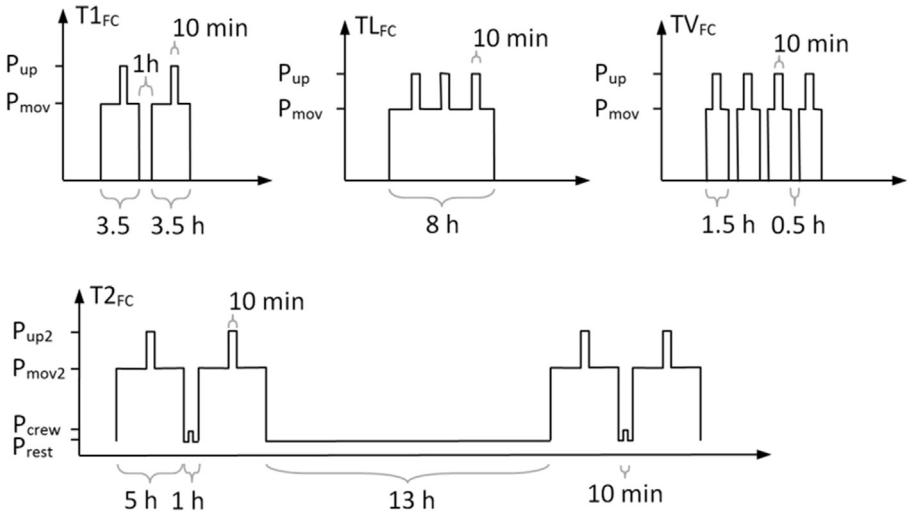

Fig. 10 – Power profile adopted for 14-days load cycles tests.

Table 16 – Calculated power levels of power profiles.

P	Power % wrt nom.	Power FC [W]	Represented power [W]
P_{up2}	152	1520	12,800
P_{up}	136	1360	11,421
P_{mov2}	100	1000	8400
P_{mov}	84	840	7021
P_{crew}	29	290	2400
P_{rest}	17	170	1400

Inclined Plane tests, conducted under constant current (80 A, 500 mA/cm^2) have produced a small difference in performance. During the experimental activity carried out at 45° and −45°, an average voltage of 15.48 V and 15.53 V (corresponding to a power of 1238.40 W and 1242.40 W) has been respectively obtained. In case of 90° and −90° inclination, an average voltage of 15.16 V and 14.88 V has been recorded (corresponding to a power of 1212.80 W and 1190.40 W). The −90°/+90° inclination led always to MEA failure, indicating that these configurations could be critical for stack operation. The MEA failure is characterized by an initial slight voltage decrease followed by a dramatic drop. In Fig. 13(a) the voltage trend of a pin-holed MEA is shown. The cell operated quite stably for at least 690 s then the voltage started to decrease for a further 300 s until it abruptly dropped to 0 V Fig. 13(b) depicts the damaged MEA after stack disassembling:

The 14-days cycle tests, has been carried out at in the following operative conditions (RH 75% t lower current density (300 mA/cm^2), the results are listed in Table 18:

The tests have been performed successfully without any appreciable degradation with a recorded efficiency of 55% at nominal power. Fast response at load variation has been recorded and higher power than expected has been observed. Cell voltages have been uniformly distributed along each fuel cell stack leading the two stacks to have a similar behaviour under cyclic tests.

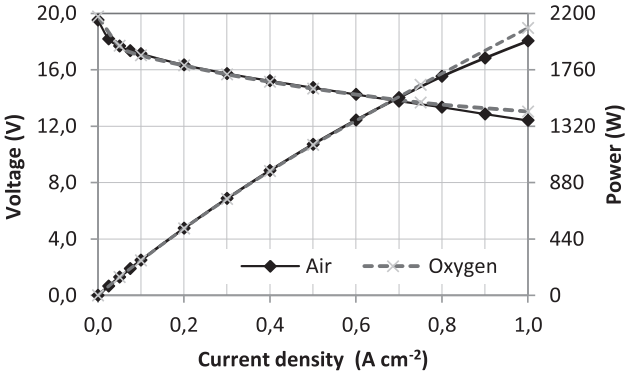

Fig. 11 – *I*–*V* polarization curves comparison, base –line H_2/Air, $T = 80$ °C $p = 3$ bar_{abs}, H_2/Air stoich. = 1.5/2.0 RH% H_2/Air = 100/100, with oxygen H_2/O_2 $T = 75$ °C $p = 3$ bar_{abs}, H_2/O_2 stoich. = 1.5/2, H_2/O_2 RH% = 50/50.

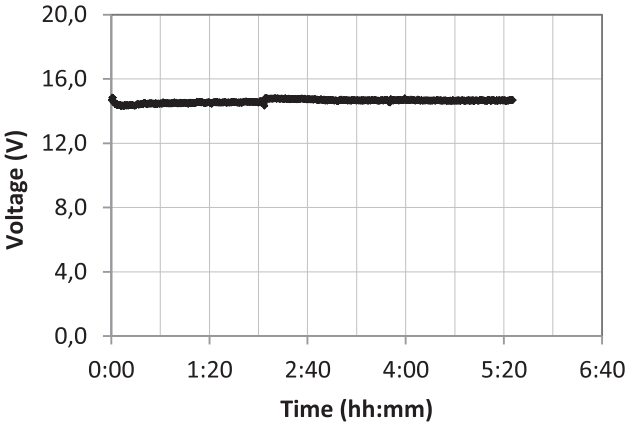

Fig. 12 – Time test (constant current load, 80 A) H_2/O_2, $T = 75$ °C $p = 3$ bar_{abs}, H_2/O_2 stoich. = 1.5/2.0, H_2/O_2 RH % = 50/50.

Test on BSA configuration

In case of stand-alone configuration, during the time test conducted under a constant load of 300 mA/cm^2, an average voltage of 15.04 V has been recorded, corresponding to a power of 721.92 W, with a voltage decay of 152.79 mV/h, as Fig. 14 shows:

The recorded difference in voltage decay, higher in case of BSA, is related to the different humidification device here adopted. In this breadboard configuration, the exhausted reactants pass through a water trap and then re-injected in the inlet stream. Thus the gas stream approaching the fuel cell stack have a temperature and a water content as resulting by the 'quasi' adiabatic mixing.

During the tests numerous failures of the recirculation compressors have been observed, identifying these devices as critical for the system reliability.

Test on BCL configuration

In closed-loop configuration the Breadboard has been tested under 10 successful runs, using the Hydrogen regenerated each time by the electrolyzer. Tests have been conducted by setting a current of 48 A (300 mA/cm^2), and monitoring the

Table 17 – Composition of the adopted operative plans.

Nominal representative T1 operative profile	$T1_{FC}$	$T1_{FC}$	$T1_{FC}$	$T1_{FC}$	$T1_{FC}$	$T1_{FC}$	$T1_{FC}$	$T2_{FC}$	$T2_{FC}$
Long duration travelling representative operative profile	TL_{FC}	TL_{FC}	TL_{FC}	TL_{FC}	TL_{FC}	TL_{FC}	TL_{FC}	$T2_{FC}$	$T2_{FC}$
Multiple quick variations travelling representative operative profile	TV_{FC}	TV_{FC}	TV_{FC}	TV_{FC}	TV_{FC}	TV_{FC}	TV_{FC}	$T2_{FC}$	$T2_{FC}$
Day	1	2	3	4	5	6	7	8	9

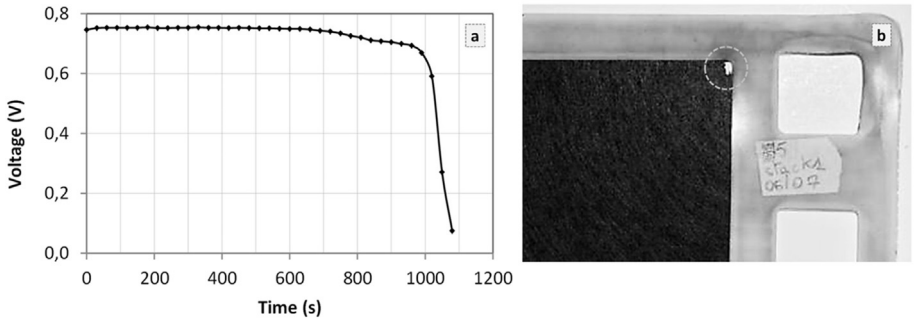

Fig. 13 – Voltage behaviour during MEA failure (a) an image of a holed MEA after stack operation in inclined plane tests (b).

stack voltage. Fresh MEAs have been used for this test, then a performance stability has been reached after the first three runs (r1 to r3) where the power showed an increasing trend. Following runs (r4 to r10) have shown a stable behaviour of the stack, the recorded average power has been in the range of 761 W (r7) – 777 W (r10), with a variation of mean power of about 2%. The stack performance is comparable with that in the previous tests. In Fig. 15 the recorded profiles are reported:

Conclusions

The proposed study has been useful to evaluate the feasibility of FC technology in space applications, in particular for a lunar base power plant and a pressurized lunar rover. The trade-off analysis allowed the best technology to be chosen. It resulted in a discrete regenerative fuel cell system, with a PEM - based fuel cell and electrolyser, using hydrogen and oxygen as reactants stored in high pressure gas cylinders. On the basis of the trade–off activity, considering the requirements of the future human exploration of the moon, the LPPE and PLR power and energy demands have been defined, resulting in a maximum power of EPM system of 4.9 kW for LPPE, 8.4 kW for PLR and a correspondent energy level of 320 kWh for LPPE, 220 kWh for PLR. The defined level of power and energy has been the input parameters of the designed and manufactured fuel cell stack breadboards. The tests performed on the three breadboard configurations have yielded encouraging results. The FC stacks produced a good performance during *I–V* curves in terms of voltages and power with a peak power of 2086 W (651.87 mW/cm^2) at 1000 mA/cm^2 and 1173 W (366.56 mW/cm^2) at 500 mA/cm^2. Time test confirmed the performances obtained with the *I–V* curve, under a constant load of 80 A (500 mA/cm^2) an average stack voltage of 14.61 V (averaged cell voltage = 0.73 V) has been recorded (1174 W corresponding to 366.87 mW/cm^2). Inclined plane tests, have produced a small difference in performance. At 45° and −45°,

Table 18 – 14-days cycle tests results.

	Power level	Power wrt nom. %	Expected power [W]	Recorded power [W]	Eff. %
$T1_{FC}$	P_{up}	136	950	1053	54
	P_{mov}	84	590	678	56
TL_{FC}	P_{up}	136	950	1048	54
	P_{mov}	84	590	676	56
TV_{FC}	P_{up}	136	950	1042	54
	P_{mov}	84	590	674	56
$T2_{FC}$	P_{up2}	152	1060	1148	53
	P_{mov2}	100	700	789	55
	P_{crew}	29	200	248	60
	P_{rest}	17	120	148	61

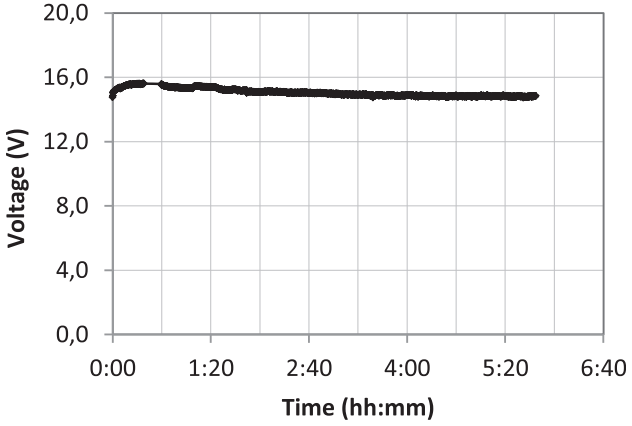

Fig. 14 – BSA, Time test (constant current load, 48 A) H_2/O_2, $T = 75$ °C $p = 3$ bar_{abs}, H_2/O_2 stoich. = recirc. H_2/O_2 RH % = recirc.

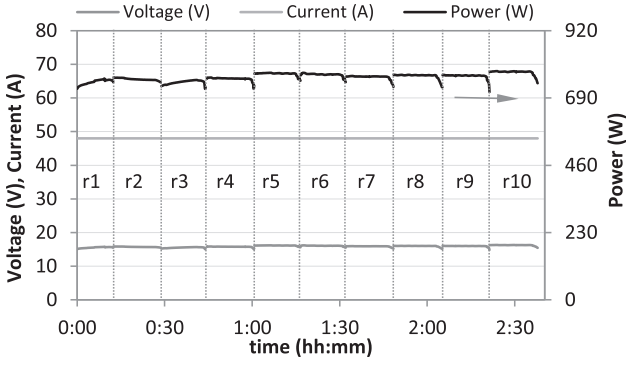

Fig. 15 – BCL, results of the 10 performed runs (constant current load, 48 A) H_2/O_2, $T = 75$ °C $p = 3$ bar_{abs}, H_2/O_2 stoich. = recirc. H_2/O_2 RH% = recirc.

an average stack voltage of 15.48 V and 15.53 V has been recorded (averaged cell voltage = 0.774 V; 0.776 V) corresponding to 1238.40 W (387 mW/cm^2) and 1242.40 W (388.25 mW/cm^2) respectively. On the other hand 90° and −90°, an average voltage of 15.16 V and 14.88 V has been observed (averaged cell voltage = 0.758 V; 0.744 V), corresponding to 1212.80 W (379 mW/cm^2) and 1190.40 W (372 mW/cm^2). Among the results, several criticalities have been identified. The −90°/+ 90° inclination tests led to MEA failure, indicating that these configurations could be critical for stack operation. For the Stand Alone configuration, the identified criticalities are related to the recirculation compressor, that has suffered from numerous failures during the operation. In conclusion, the study has demonstrated the high performances of the developed PEM based system to be used in future lunar human exploration missions.

Acknowledgements

This study has been funded by European Space Agency (grant number 4000101742/10/NL/JC).

The authors are very grateful to Dr. Antonino S. Aricò for kindly helping in the revision of the manuscript and to Dr. Fabio V. Matera for his support on stand – alone breadboard assembling and control software development.

REFERENCES

[1] Statement of work energy provision and management study. European Space Agency; 2010. rev. 3.
[2] Surampudi S. Overview of the space power conversion and Energy storage technologies. http://www.lpi.usra.edu/sbag/meetings/jan2011/presentations/day1/d1_1200_Surampudi.pdf.
[3] Surampudi R. Overview of Energy storage technologies for space application. In: 42nd power sources conference Philadelphia United States; 2006.
[4] www.nasa.gov.
[5] Sone Y. A 100-W class regenerative fuel cell system for lunar and planetary missions. J Power Sources 2011;196:9076–80.
[6] Burke KA. Fuel cells for space science applications. In: First international Energy conversion engineering. Conference Portsmouth, Virginia; August 17–21, 2003.
[7] Pérez - Davis ME, Loyselle PL, Hoberecht MA, Manzo MA, Kohout LL, Burke KA, et al. Energy storage for aerospace applications. In: 36th intersociety Energy conversion engineering conference, Savannah, United States; 2001.
[8] www.esa.int.
[9] Fisackerly R, Reimers C-J, Pradier A. Exploration system technology aspects in the exploration programme of the European Space Agency. Acta Astronaut 2006;59:3–12.
[10] Bonnet R-M, Swings PJ. The Aurora programme; 2004. ESA Publ. Div., no. 31.
[11] Programme E. The European space exploration programme. ESA Bull 2003;115:34–9.
[12] Messina P, Gardini B, Sacotte D, Di Pippo S. The Aurora programme. ESA Bull 2006;126.
[13] The MELiSSA project; 2007. http://www.esa.int/SPECIALS/Melissa/SEMU54V681F_2.html.
[14] Gehrke H, Heyn J, Dietrich G. Fuel cell systems for space applications in Europe. Acta Astronaut 1988;17:531–8.
[15] Sone Y. Fuel cell development for space applications: fuel cell system in a closed environment. J Power Sources 2004;1372:69–276.
[16] Lucia U. Overview on fuel cells. Renew Sustain Energy Rev 2014;30:164–9.
[17] Mekhilef S, Saidur R, Safari A. Comparative study of different fuel cell technologies. Renew Sustain Energy Rev 2012;16:981–9.
[18] Smolinka T. Water electrolysis. In: Encyclopedia of electrochemical power sources; 2009. pp. 394–413.
[19] Carmo M, Fritz DL, Mergel J, Stolten D. A comprehensive review on PEM water electrolysis. Int J Hydrogen Energy 2013;38:4901–34.
[20] Sakintuna B, Lamaridarkrim F, Hirscher M. Metal hydride materials for solid hydrogen storage: a review. Int J Hydrogen Energy 2007;32:1121–40.
[21] Lim KL, Kazemian H, Yaakob Z, Daud WRW. Solid-state materials and methods for hydrogen storage: a critical review. Chem Eng Technol 2010;33:213–26.
[22] Shapiro D, Duffy J, Kimble M, Pien M. Solar-powered regenerative PEM electrolyzer/fuel cell system. Sol Energy 2005;79:544–50.
[23] www.globalspaceexploration.org/wordpress.
[24] Frischauf N, Acosta-Iborra B, Harskamp F, Moretto P, Malkow T, Honselaar M, et al. The hydrogen value chain: applying the automotive role model of the hydrogen economy in the aerospace sector to increase performance and reduce costs. Acta Astronaut 2013;88:8–24.
[25] Barbir F, Molter T, Dalton L. Efficiency and weight trade-off analysis of regenerative fuel cells as energy storage for aerospace applications. Int J Hydrogen Energy 2005;30:351–7.
[26] Bents BDJ, Scullin VJ, Glenn N, Chang BJ, Johnson DW, Garcia CP, et al. Hydrogen-oxygen PEM regenerative fuel cell development at Nasa Glenn Research Center. Fuel Cells Bull 2006;2006:12–4.
[27] Squadrito G, Giacoppo G, Barbera O, Urbani F, Passalacqua E, Borello L, et al. Design and development of a 7 kW polymer electrolyte membrane fuel cell stack for UPS application. Int J Hydrogen Energy 2010;35:9983–9.
[28] Giacoppo G, Barbera O, Carbone A, Gatto I, Saccà A, Pedicini R, et al. 1.5 kWe HT-PEFC stack with composite MEA for CHP application. Int J Hydrogen Energy 2013;38:11619–27.
[29] Squadrito G, Barbera O, Gatto I, Giacoppo G, Urbani F, Passalacqua E. CFD analysis of the flow-field scale-up influence on the electrodes performance in a PEFC. J Power Sources 2005;15:267–74.
[30] Sone Y, Ueno M, Naito H, Kuwajima S. One kilowatt-class fuel cell system for the aerospace applications in a micro-gravitational and closed environment. J Power Sources 2006;57:886–92.
[31] Chen S, Wu Y. Gravity effect on water discharged in PEM fuel cell cathode. Int J Hydrogen Energy 2010;35:2888–93.
[32] Kimball E, Whitaker T, Kevrekidis YG, Benziger JB. Drops, slugs, and flooding in polymer electrolyte membrane fuel cells. AICHE J 2008;54:1313–32.